Supporting Information

A Single Step Wet Chemical Approach to Bifunctional Ultrathin $(ZnO)_{62}(Fe_2O_3)_{38}$ Dendritic Nanosheets

Saba Latif,[a] Bilal Akram,[*b] Chaudry Sajed Saraj,[c,d] Bilal Ahmad Khan,[*a] Mudussar Ali[e] and Javeed Akhtar[f]

EXPERIMENTAL SECTION

Synthesis of FZDNSs: Initially, 259 mg ferrous chloride and 219 mg zinc acetate was dissolved into 50 mL deionized water through stirring. Then, another mixture was prepared by dissolving 210 mg urea and 378 mg sodium borohydride into 10 mL ethanol. After that, both the solutions were mixed under stirring for half an hour and then transferred into a 100 ml capacity sealed pressure tube and heated at oil bath at 100 °C for 12 hours. The formed products were then harvested through centrifugation, washed repeatedly with deionized water and ethanol, and then dried at 80 °C for 20 hours. Finally, the obtained products were annealed at 600 °C for 12 h under air atmosphere.

Synthesis of ZnO: 50 mL of 219 mg zinc acetate was dissolved in deionized water through continuous stirring. In another beaker 10 mL ethanolic solution of 210 mg urea and 378 mg sodium borohydride was prepared. Subsequently both the solutions were mixed, and the obtained mixture was transferred into a 100 ml capacity sealed pressure tube and heated at oil bath at 100 °C for 12 hours. The formed products were then harvested through centrifugation, washed repeatedly with deionized water and ethanol, and then dried at 80 °C for 20 hours. Finally, the obtained products were annealed at 600 °C for 12 h under air atmosphere.

Synthesis of Fe2O3: 50 mL of 259 mg ferrous chloride was dissolved in deionized water through continuous stirring. In another beaker 10 mL ethanolic solution of 210 mg urea and 378 mg sodium borohydride was prepared. Subsequently both the solutions were mixed, and the obtained mixture was transferred into a 100 ml capacity sealed pressure tube and heated at oil bath at 100 °C for 12 hours. The formed products were then harvested through centrifugation, washed repeatedly with

deionized water and ethanol, and then dried at 80 °C for 20 hours. Finally, the obtained products were annealed at 600 °C for 12 h under air atmosphere.

Characterization of prepared test analytes

Transmission electron microscopy (TEM) (Hitachi, H-800; operated at 200kV), scanning electron microscopy (SEM) and X-ray diffraction (Rigaku, Smartlab; operated at 40kV and 200mA, Cu Kα source) were employed to get structural characterization of synthesized test analytes. Energy Dispersive X-ray spectroscopy coupled with electron microscopy (EDX) was used to determine the elemental composition of the synthesized test analytes. The precise elemental composition and hence the precise molecular formula was estimated using inductively coupled optical emission spectroscopy (ICP-OES). The surface functional groups and successful preparation of target material was determined by applying Fourier transform infrared (FTIR) analysis using FTIR spectrometer (FTIR-2000, Bruker). The absorption properties were recorded on a UV–Vis spectrophotometer (Shimadzu-1601). Thermogravimetric analysis (TGA) was performed with Mettler Toledo TGA/SDTA851e at a heating rate of 10 °C min^{-1} from room temperature to 700 °C under air flow.

Photoreduction performance of FZDNSs

Photocatalytic performance of newly designed FZDNSs was assessed using one of the most common reaction, para-nitrophenol conversion to para-aminophenol. Photoreduction experiments were conducted using 50mL of known concentration of p-nitrophenol (1 mmol) with 50mg of nano catalyst (1mg catalyst/mL of para-nitrophenol solution). The reaction was initiated by adding 0.05 mole of $NaBH_4$ as reducing agent. The obtained reaction mixture was stirred in dark for 20 minutes to get adsorption and desorption equilibrium. After dark treatment catalyst containing reaction mixture was subject to stirring under light illumination. The progress of photoreduction reaction was monitored using UV-vis spectrophotometer at regular time intervals. While analysing the reaction progress syringe was used to get required volume of reaction solution to minimize catalyst injection. The reusability and steadiness of photocatalyst was assessed by removing and reusing the catalyst from the reaction mixture after reaction completion. Catalyst was harvested through centrifugation, washed several times with water and ethanol and oven dried prior to reuse.

Electrochemical Measurements

Electrocatalyst ink of various test analytes were obtained by first ultrasonically dispersing 5 mg of test analytes into 0.5ml of isopropyl alcohol (IPA) and 0.5ml deionized water solution followed by the addition of 50 µl of 0.5M Nafion solution.

10 µl of as prepared catalyst ink was deposited on a Carbon cloth electrode (0.6cm^2 area) to get the working electrode which was dried in air at room temperature prior to use.

Electrochemical measurements were performed on BioLogic VMP3 multichannel workstation with a three-electrode system, where a Pt wire, a catalyst loaded carbon cloth electrode, and a saturated calomel electrode (SCE) were used as counter, working and reference electrodes, respectively. The electrolytes employed during electrochemical measurements is aqueous 1M KOH solution. LSV curves were obtained by sweeping voltage in the range of -0.2 to -1.6 V vs SCE electrode with the scan rate of 10 mVs^{-1}. Expression $E_{RHE} = E_{SCE} + E_{SCE}^{0} + 0.0592 * pH$, where $E_{SCE}^{0} = 0.242\ V$, was used to translate V vs SCE to V vs reverse hydrogen electrode (RHE). WE were pre-stabilized in the electrolyte solution using several scans of cyclic voltammetry at 40mV/s before performing linear sweep voltammetry measurements. Electrochemical impedance spectra (EIS) were recorded with the biasing of working electrode at -1.4V (HER) and superimposing a small alternating voltage of 10 mV over the frequency range of 0.01Hz to 1 MHz. The CV curves were further measured in the non-Faradaic region of potential from 0.83 V to 0.91 V (vs RHE) with different scan rates (from 10 mVs^{-1} to 100 mVs^{-1}) to estimate the double layer capacitance (Cdl).

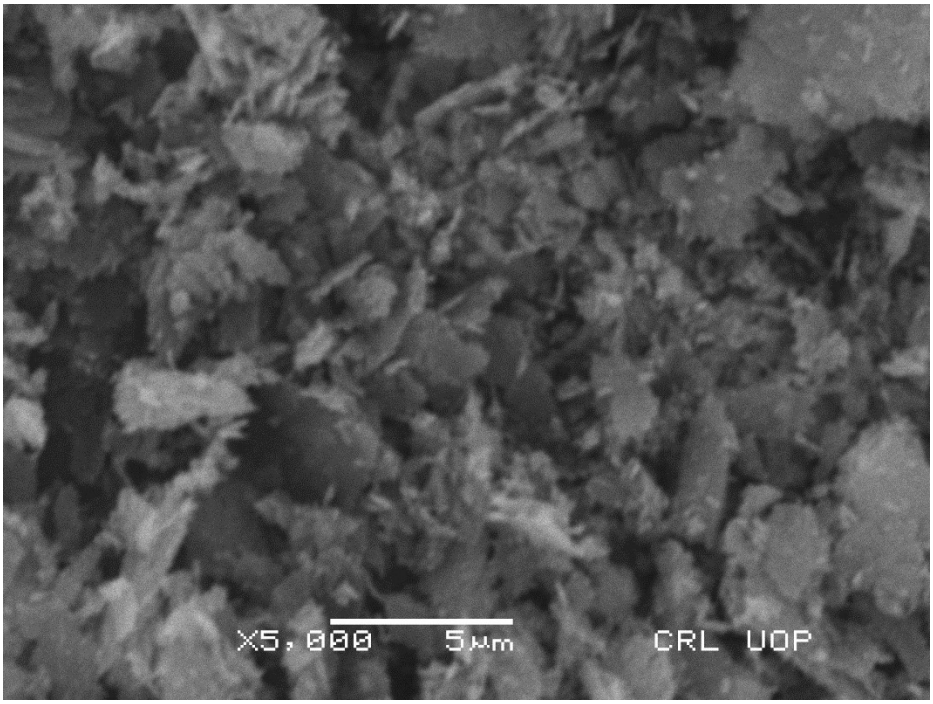

Figure S1. SEM image of FZDNSs.

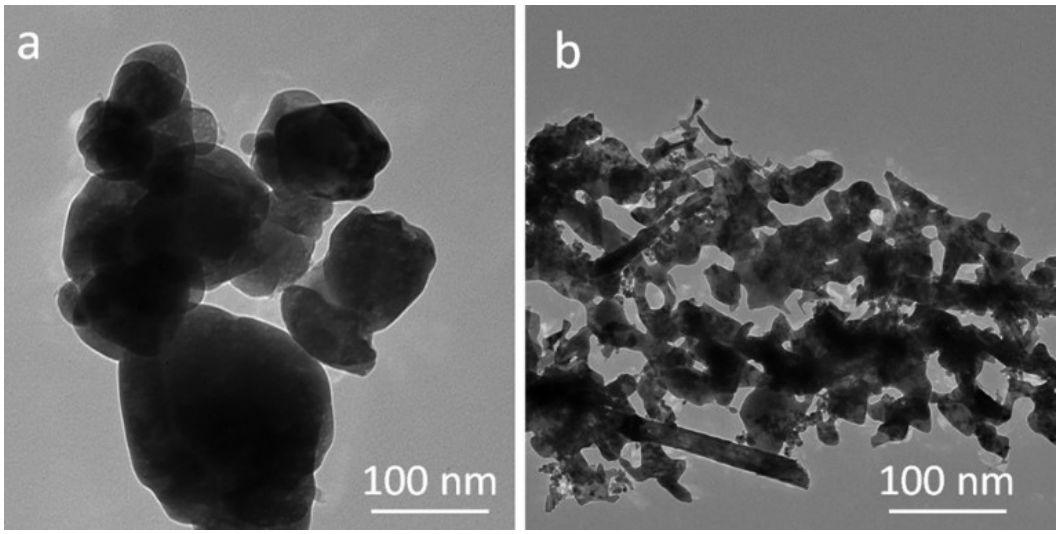

Figure S2. TEM images of a) pure ZnO and b) pure Fe_2O_3

Table S1. ICP-OES analysis results of Zn and Fe in FZDNSs.

	sample	FZDNSs
Zn	34.64	wt%
Fe	48.69	wt%

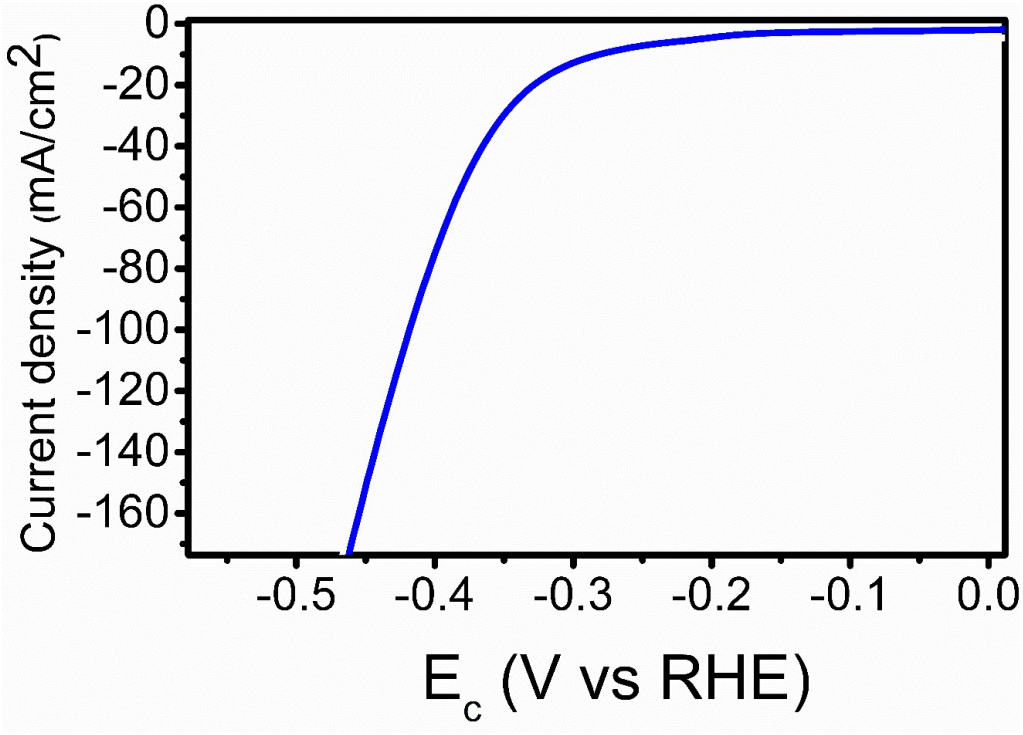

Figure S3. LSV curve of FZDNSs after CA test.

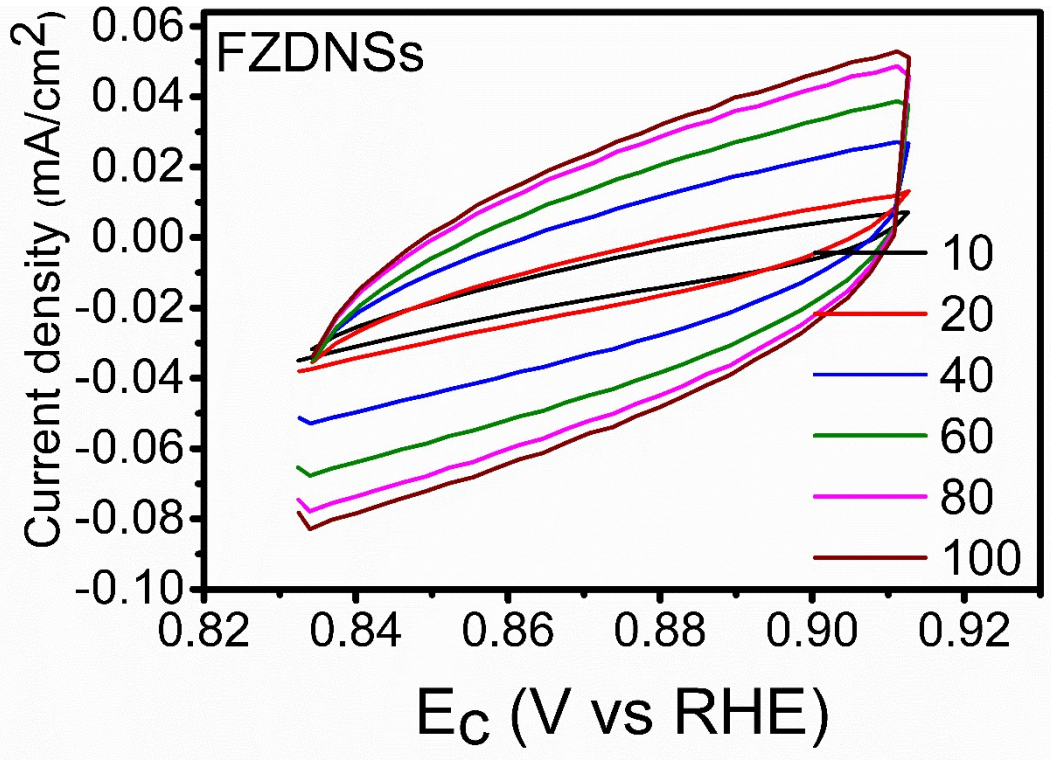

Figure S4. Cdi curves of FZDNSs.

Table S2. Comparative literature data for the reduction of 4-NP using different catalysts.

Sr No	Photocatalyst	Concentration mg/L	Loading mg	Light source	Time (min)	Efficiency %	Reference
1	Fe2O3/RGO	20	50	Visible light	120	78	01
2	Ag/In2S3/ZnO	10	50	Visible light	50	55	02
3	In2S32%GR	10	10	Visible light	120	80	03
4	In2S3–3%CNT	10	40	Visible light	60	97	04
5	60%In2S3/α-Fe2O3	10	40	Visible light	100	95	05
6	FZDNSs	10	50	Visible light	50	96	This work

Table S3. Performance comparison of FZDNSs with previously reported materials towards HER application.

Sr. No	Electrocatalyst	Electrolyte HER	η value at 10 mA cm^{-2}	Tafel slope mV/dec^{-2}	Reference
1	P-Co3O4	1 M KOH	120 mV	52.0	6
2	Fe-P/Ti	1 M KOH	95 mV	-	7
3	Fe-P	1 M KOH	194 mV	75.0	8
4	Fe CoO-NF	1 M KOH	205 mV	118.0	9
5	Ni CoFeP/C	1 M KOH	149 mV	89.0	10

6	Ni-Fe2O3	1 M KOH	310 mV		11
7	Ni-FeP/C	1 M KOH	95 mV	72	12
8	N-FeP	1 M KOH	226 mV	84.8	13
9	NiCoFeO	1 M KOH	131 mV	56	14
10	Mn-FeO	1 M KOH	173 mV	95	15
11	13 Ni-Fe/NF	1 M KOH	142 Mv	133.3	16
12	Co 0.75 Fe 0.25-NC	1 M KOH	202 mV	67.96	17
13	Co 0.59 Fe 0.41 P	1 M KOH	92 mV	72	18
14	Fe3+Ni@NCF	1 M KOH	219 mV	109.9	19
15	P-doped Fe2O3/ZnO nanotubes	1 M KOH	139 mV	104	20
16	N-doped Fe2O3/ZnO nanotubes	1 M KOH	312 mV	315	20
17	ZnO NPs	1 M KOH	647 mV	91	This work
18	Fe2O3 NPs	1 M KOH	281 mV	79	This work
19	FZDNSs	1 M KOH	182 mV	64	This work

References

1. B.S. Mohan, K. Ravi, R.B. Anjaneyulu, G.S. Sree, K. Basavaiah, Phys. Condens. Matter, 2019, 553 190–194.

2. J.W. Wei, S.M. Wei, N. Chang, H.T. Wang, J.M. Zhang, Nanotechnology, 2021, 32, 10, 105706.

3. M.Q. Yang, B. Weng, Y.J. Xu, Langmuir, 2013, 29, 33, 10549–10558.

4. M.Q. Yang, B. Weng, Y.J. Xu, J. Mater. Chem. A, 2014, 2, 6, 1710–1720.

5. L. Fang, R. Jiang, Y. Zhang, R. M. Munthali, X. Huang, X. Wu, Z. Liu, J. Solid Stat. Chem., 2021, 303, 122461.

6. Z. Xiao, Y. Wang, Y.-C. Huang, Z. Wei, C.-L. Dong, J. Ma, S. Shen, Y. Li and S. Wang, Energy Environ. Sci., 2017, 10, 2563–2569.

7. X. Zhao, Z. Zhang, X. Cao,J. Hu, X. Wu, A. Y. R. Ng, G. P. Lu and Z. Chen, Appl. Catal.

B Environ., 2020, 260, 118156.

8. C. Y. Son, I. H. Kwak, Y. R. Lim and J. Park, Chem. Commun., 2016, 52, 2819–2822.

9. H. A. Bandal, A. R. Jadhav, A. H. Tamboli and H. Kim, Electrochim. Acta, 2017, 249, 253–262.

10. X. Wei, Y. Zhang, H. He, L. Peng, S. Xiao, S. Yao and P. Xiao, Chem. Commun., 2019, 55, 10896–10899.

11. L. Zeng, K. Zhou, L. Yang, G. Du, L. Liu and W. Zhou, ACS Appl. Energy Mater., 2018, 1, 6279–6287.

12. S. Xu, H. Zhao, T. Li, J. Liang, S. Lu, G. Chen, S. Gao, A. M. Asiri, Q. Wu and X. Sun, J. Mater. Chem. A, 2020, 8, 19729–19745.

13. J. Huang, J. Han, T. Wu, K. Feng, T. Yao, X. Wang, S. Liu, J. Zhong, Z. Zhang, Y. Zhang and B. Song, ACS Energy Lett., 2019, 3002–3010.

14. Z. Ge, B. Fu, J. Zhao, X. Li, B. Ma and Y. Chen, J. Mater. Sci., 2020, 55, 14081–14104.

15. M. Wang, Y. Tuo, X. Li, Q. Hua, F. Du and L. Jiang, ACS Sustain. Chem. Eng., 2019, 7, 12419–12427.

16. Z. Zhang, Y. Wu and D. Zhang, Int. J. Hydrogen Energy, 2022, 47, 1425–1434.

17. X. Feng, X. Bo and L. Guo, J. Power Sources, 2018, 389, 249–259.

18. X. Wen and J. Guan, Appl. Mater. Today, 2019, 16, 146–168.

19. Z. Zhang, L. Cong, Z. Yu, L. Qu and W. Huang, Mater. Today Energy, 2020, 16, 100387

20. P. M. Ganje, H. A. Bandal and K. Hern, *Sustainable Energy & Fuels*, 2022, **6**, 5579-5590.